LBNL-47428

Article submitted to

Journal of Physics D: Applied Physics.

Improved Tribology of Tool Steel by Zirconium Ion Implantation

N. Akbas†, A. Oztarhan‡, O.R. Monteiro§ and I.G. Brown§

† Celal Bayar University, Manisa 45010, Turkey

‡ Yuzey Teknolojileri San. Ve Tic. A.S. Izmir, Turkey

§ Lawrence Berkeley National Laboratory, Berkeley CA 94720, USA

February 2001

Contact Author: Dr. Othon R. Monteiro
Lawrence Berkeley National Laboratory
Mail Stop 53-004
One Cyclotron Rd.
Berkeley, CA 94720 USA
e-mail: ORMonteiro@lbl.gov
FAX: (510) 486-4374

This work was supported by the U.S. Department of Energy, under contract No. DE-AC03-76SF00098.

Improved Tribology of Tool Steel by Zirconium Ion Implantation

N. Akbas†, A. Oztarhan‡, O.R. Monteiro§ and I.G. Brown§

† Celal Bayar University, Manisa 45010, Turkey

‡ Yuzey Teknolojileri San. Ve Tic. A.S. Izmir, Turkey

§ Lawrence Berkeley National Laboratory, Berkeley CA 94720, USA

Abstract

AISI D3 tool steel was ion implanted with zirconium and the improvement in surface tribological properties investigated. The Zr ion implantation was done using a metal vapor vacuum arc broad-beam ion source, with a mean ion energy of 130 keV and at doses of 3.6 x 10^{16}, 5 x 10^{16} and 1 x 10^{17} ions/cm^2. Wear, friction and hardness of the implanted samples were measured and compared to the performance of unimplanted steel. The wear resistance was increased by about a factor of two, the friction remained about the same or was possibly increased by a small amount, and the hardness was improved by a factor of five or more by the ion implantation. We also investigated the effect on the Zr implantation profile of the multi-component energy distribution of the ion beam used here.

1. Introduction

Ion implantation is an effective method for improving the surface physical and mechanical properties of materials, such as wear, hardness and corrosion resistance [1-4]. While initially developed for doping semiconductor devices, the use of ion implantation has experienced a substantial increase in recent years as a tool for the surface modification of metals, ceramics and other engineering materials. In particular, improvement in the surface properties of hard tool steel by ion implantation has been investigated by a number of workers [5-8]. The Mevva (*me*tal *v*apor *v*acuum *a*rc) ion source has evolved to be a relatively simple and low-cost surface modification tool [9-14], and has been developed by a growing number of research groups around the world for carrying out metal ion implantation into a range of materials [1,15-17]. We describe here some observations we have made of the changes in surface wear, friction and hardness of AISI D3 tool steel subsequent to implantation with Zr ions using a Mevva ion implantation facility. We report our measurements and discuss the results in light of the current literature.

2. Experimental

Small coupons of AISI D3 tool steel (2 – 2.35% C; 0.6% Mn; 0.6% Si; 11 – 13.5% Cr; 0.3% Ni; 1% W; 1% V) were prepared to a mirror finish using a succession of SiC grinding papers followed by polishing in a diamond slurry down to 1 μm particle size. The samples were cleaned in an ultrasonic bath with acetone and ethanol. Ion implantation was performed using a broad-beam vacuum arc ion source that formed a Zr ion beam of pulse length of 250 μs at a repetition rate of several pulses per second. Beam extraction voltage was 50 kV, corresponding to a mean ion energy of about 130 keV since the mean charge state for Zr ion is 2.6 for the vacuum arc plasma [11,18]. Beam current was about 200 mA as measured by a

radially-moveable, 5-cm diameter, magnetically suppressed, Faraday cup located 65 cm downstream from the source; this corresponds to a current density of about 20 mA/cm^2 during the pulse-on time and to a time-averaged ion beam current density of ~5 μA/cm^2. The steel coupons to be implanted were introduced into the beam path on a water-cooled target holder located adjacent to the Faraday cup. Background gas pressure in the implantation chamber was kept below about 2 x 10^{-6} Torr. Details of the ion source operation and the implantation set-up have been described elsewhere [11,12].

The implantation dose incident upon the target is estimated from the known beam current and the number of beam pulses that are accumulated in an implantation run. Because of a number of factors, particularly that the radial distribution of ion beam current density is not flat, this estimate of applied dose is accurate only to within a factor of two. The actual retained dose and the depth distribution of the implanted species is determined by Rutherford backscattering spectroscopy (RBS) of the implanted samples using 2 MeV He^+ ions.

Wear measurements were performed using a pin-on-disc tribometer (CSEM) with an Al_2O_3 ball (6 mm diameter) under dry conditions using a load of 1 N and a constant speed of 0.02 ms^{-1}. A total of 1000 turns were made before each test was discontinued. The temperature of the substrate during the wear tests was 22 ^oC. Coefficient of friction was recorded during the wear testing using the same equipment. The profiles of the wear tracks were characterized with a profilometer (Mahr Pertometer PRK) after the end of each test. Microhardness was measured using a CSEM nanohardness tester with a Vickers indenter and normal loading from 5 to 300 mN. This corresponds to determining microhardness at several different depths.

3. Results and Discussion

The RBS-derived depth profiles for samples implanted at three different doses are shown in Figure 1(a); the retained Zr doses are 3.6 x 10^{16}, 5 x 10^{16} and 1 x 10^{17} ions/cm^2. The maximum in Zr concentration for all three doses lies 2.3 x 10^{17} atoms cm^{-2} below the surface, or approximately 300 Å. We have also calculated the expected implantation depth profiles using the dynamic TRIM (T-dyn) Monte-Carlo computer code [19-22]. In this calculation the experimentally measured Zr ion charge state distribution 11,18] was used, with the particle current fractions for Zr^{2+},Zr^{3+}, and Zr^{4+} being 47%, 45%, and 8% (mean charge state 2.6). This corresponds to an ion beam with energy components at 100 keV, 150 keV and 200 keV in the same proportions. This broad energy distribution leads to a broader implantation depth profile than would be the case for a single ion energy. The result of the simulation for a dose of 3.6 x 10^{16} cm^{-2} is shown in Figure 1(b) and can be compared to the experimentally measured profile shown in Figure 1(a) (top figure). The calculated and the measured profiles agree within the accuracy of the measurements.

The microstructure of the AISI D3 steel coupon that had been implanted to the highest dose was characterized using scanning electron microscopy with ESCA. An SEM image with elemental profiles is shown in Figure 2. It can be seen that the sample consists primarily of a chromium carbide phase dispersed in a carbon-containing iron-rich phase, and the Zr appears to be uniformly distrbuted across the different phases.

We measured the hardness of the implanted samples and of an unimplanted sample. Since the dimension of the dispersed phase is greater than the indenter impression used to determine the hardness, random selection of the indenter position for hardness measurements would lead to a large scatter in the results. We therefore chose to perform the indentations only on regions showing a carbidic phase. Hardness was then determined for different

applied loads, corresponding to different indentation depths. The results are shown in Figure 3, where the Vickers Hardness (H_V) is plotted as a function of the applied load in mN. These results can be comnpared to typical Vickers Hardness values for chromium carbides that are in the range 1200 to 1800 [23] depending on the composition and on the structure. The increase in hardness for very low applied loads, as seen in Figure 3, can be associated with a hardening efect resulting from the Zr implantation. When larger loads are used, the probed region is larger and the contribution from depths greater than the implanted range becomes significant. The measurements taken with the smallest load are the closest to the actual surface hardness. Finally we note that the results show no significant dependence of the hardness on the implantation dose, for the range of doses investigated here. Ion implantation can promote hardening by three mechanisms: defect generation, solution hardening and precipitate hardening. We have used X-ray diffraction in glancing angle mode to look for the presence of precipitates, but no evidence of precipitation was found even for the largest implantation dose. In general, there is a direct correlation between solution hardening and defect concentration with dose, up to a maximum dose that leads to precipitation.

Results of wear test measurements of the implanted samples and an unimplanted sample are shown in Figure 4. The wear of the implanted material is about a factor of two less than the unimplanted material. The wear decreases with increasing implantation dose up to 5 x 10^{16} cm^{-2}, and then increases as the dose is increased to 1 x 10^{17} cm^{-2}.

The coefficient of friction was monitored during the ball-on-disc tests of the implanted and unimplanted samples, and was observed to remain approximately constant throughout the test duration. For the unimplanted material the coefficient of friction was 0.75, and for the three implanted samples, in order of increasing dose, 0.77, 0.84 and 0.76. We conclude that the friction coefficients for all samples are the same at about 0.80 ± 0.05, within the

significance of the measurements. Note however, the sample with the highest measured friction coefficient was also the hardest, and showed the lowest wear.

5. Conclusions

We have investigated some of the tribological characteristics of Zr-implanted AISI D3 tool steel and compared with unimplanted steel. The wear resistance was increased by about a factor of two, the friction remained about the same, and the hardness (measured for the chromium carbide phase only, and not from the matrix) was improved by a factor of five or more by the ion implantation.

Acknowledgement

One of us (NA) is grateful to TUBITAK (The Scientific and Technical Research Council of Turkey) for support as a visiting scientist at Lawrence Berkeley National Laboratory. This work was supported by the U.S. Department of Energy, under contract No. DE-AC03-76SF00098.

References

1. See, for instance, the proceedings of the biennial conferences on Ion Beam Modification of Materials (IBMM), published in *Nucl. Instrum. Meth. Phys. Res.,* and on Surface Modification of Materials by Ion Beams (SMMIB), published in *Surf. Coat. Technol.*
2. Caudron E and Buscail H 2000 Comparison of the oxidation resistances of yttrium implanted low manganese and low manganese-carbon steels at high temperature *Applied Surface Science* **158** 310-29
3. Noli F, Misaelides P, Giorginis G, Baumann H and Hatzidimitriou A 1995 The effect of Zr-implantation on the thermal oxidation and aqueous corrosion of AISI 321 stainless steel *Nucl. Instrum. Meth Phys Res* **B95** 197-207
4. Rueck D M, Boos D and Brown I G 1993 Improvement in wear characteristics of steel tools by metal ion implantation *Nucl. Instrum. Meth. Phys. Res.* **B80/81** 233
5. Lee E H, Byun T S, Hunn J D, Hashimoto N and Farrell K 2000 A method to study deformation mechanisms for irradiated steels using a disk-bend test *J. Nucl. Materials* **281** 65-70
6. Jahrling F, Rueck D M and Fuess H 1999 Hardness, wear and microstructure of carbon implanted AISI M2 high speed steel *Surf. Coat. Technol.* **111** 111-18
7. Umehara, N, Bong-Ho Moon and Kato K 1998 Microscopic wear mechanisms of Ti ion-implanted 1C-3Cr steel *Wear* **218** 210-15
8. Byeli A V, Lobodaeva O V, Shykh S K and Kukareko V A 1995 Solid-state amorphization of a tool steel by high-current-density, low-energy nitrogen ion implantation *Nucl. Instrum. Meth. Phys. Res.* **B103** 533-6
9. Brown I G, Galvin J E and MacGill R A 1985 High current ion source *Appl. Phys. Let*t. **47** 358-60

10. Brown I G and Oks E M 1997 Vacuum arc ion sources – a brief historical review *IEEE Trans. Plasma Sci.* **25** 1222-28
11. Brown I G 1994 Vacuum arc ion sources *Rev. Sci. Instrum*. **65** 3061-81
12. Brown I G, Dickinson M R, Galvin J E, Godechot X and MacGill R A 1992 Versatile high current metal ion implantation facility *Surf. Coat. Technol.* **51** 529-33
13. See, for instance, *Rev. Sci. Instrum.* 1994 **65** 3061-3139. This journal issue contains a review of vacuum arc ion sources and a collection of papers on this topic by a number of authors from laboratories around the world.
14. See, for instance, the proceedings of the biennial International Conferences on Ion Sources: *Rev. Sci. Instrum.* 1990 **61**(1) 221-666; 1992 **63**(4) 2351-2912; 1994 **65**(4) 1039-1484; 1996 **67**(3) 867-1423; 1998 **69**(2) 613-1206; 2000 **71**(2) 603-1242.
15. Miao W, Tao K, Li B and Liu B X 2000 Formation of DO_{23}-Al_3Zr by Zr ion implantation using a metal vapour vacuum arc ion source *J. Phys. D: Appl. Phys.* **33** 2300-03
16. Huang Nacan, Wu Qibai, Hu Shejun, Xu Chenghui, Shi Weidong and Liu Zhenmin 2000 Surface improvement of 65Nb steel by Ti and Y ion implantation *Acta Metallurgica Sinica* **36** 634-37
17. Shi Weidong and He Feizhou 1996 MEVVA ion source and its applications *Nuclear Techniques* **19** 249-56
18. Brown I G and Godechot X 1991 Vacuum arc ion charge state distributions *IEEE Trans. Plasma Sci.* **19** 713-17
19. Ziegler J F, Biersack J P and Littmark U 1985 *The Stopping and Range of Ions in Matter* (New York: Pergamon).
20. Biersack J P, Berg S and Nender C 1991 T-Dyn Monte carlo simulations applied to ion assisted thin film processes *Nucl. Instrum. Meth. Phys. Res.* **B59/60** 21

21. J.P. Biersack 1987 Three-dimensional distributions of ion range and damage including recoil transport *Nucl. Instrum. Meth.* **B19/20** 32

22. J.P. Biersack 1987 Computer simulations of sputtering *Nucl. Instrum. Meth.* **B27** 21

23. Pierson H 1996 *Handbook of Refractory Carbides and Nitrides* (Noyes: Park Ridge NJ)

Figure Captions

Fig. 1 (a) Zr depth profiles measured by RBS, for three doses as indicated;

(b) Zr depth profile calculated using T-Dyn, for a dose of 3.6×10^{16} cm^{-2}.

Fig. 2 SEM microprobe analysis showing microstructure and composition.

Fig. 3 Hardness as a function of applied load

Fig. 4 Wear for implanted and unimplanted samples.

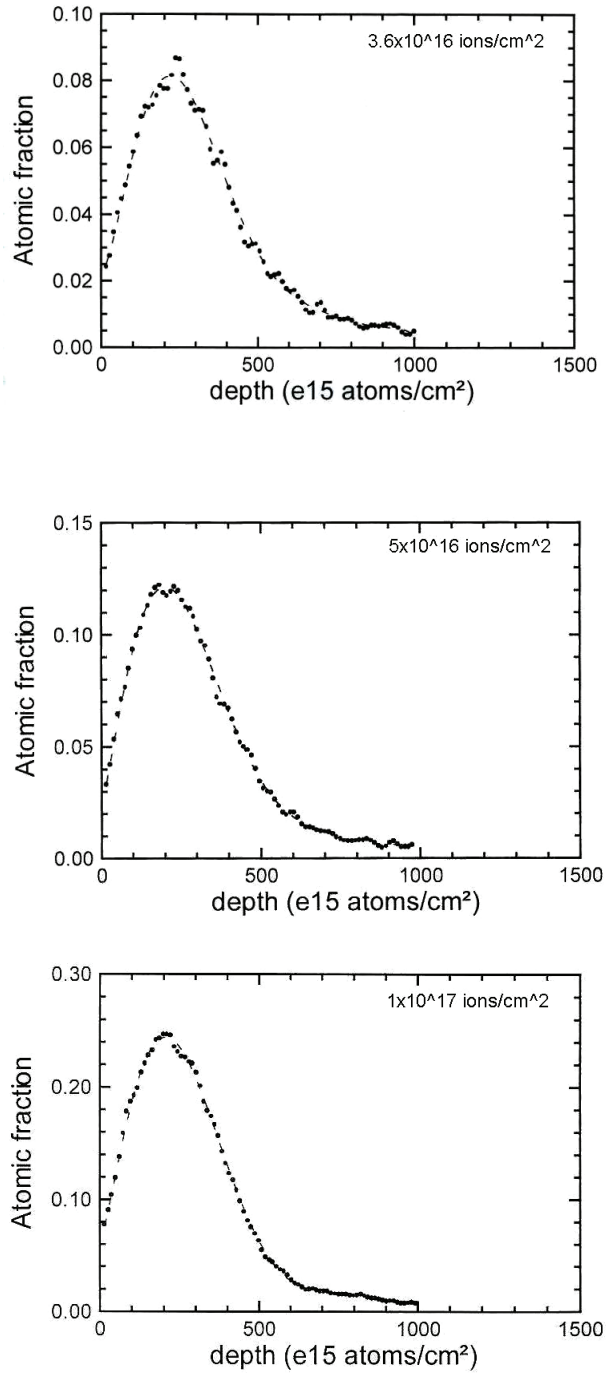
3.6x10^16 ions/cm^2
Atomic fraction
depth (e15 atoms/cm²)
5x10^16 ions/cm^2
Atomic fraction
depth (e15 atoms/cm²)
1x10^17 ions/cm^2
Atomic fraction
depth (e15 atoms/cm²)

Figure 1(a)

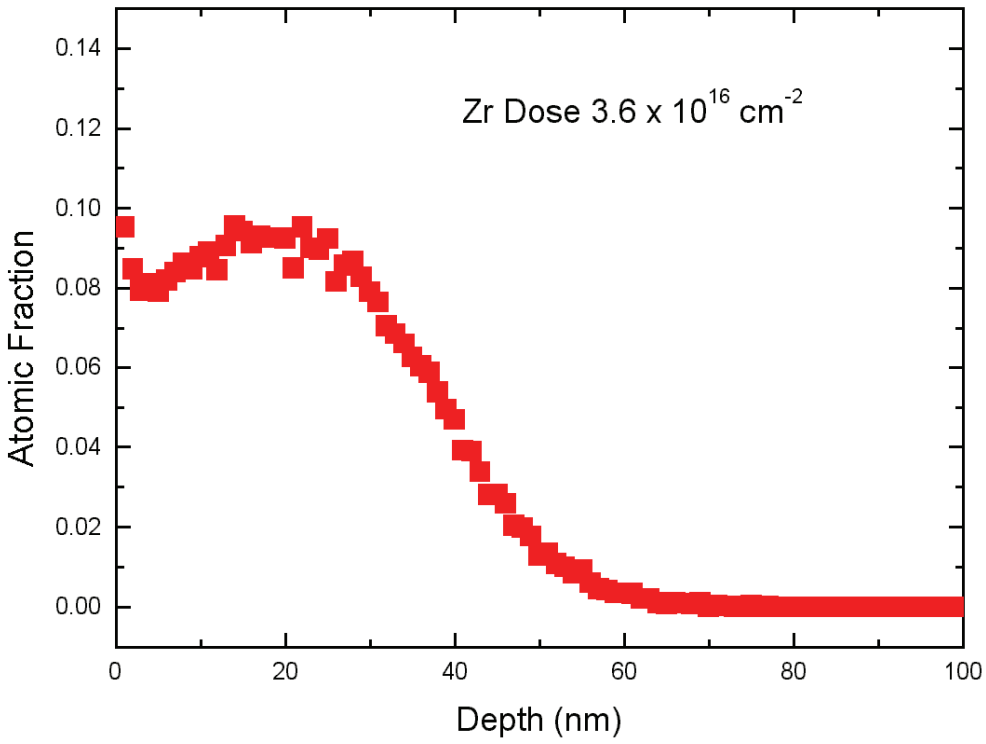
Zr Dose 3.6 x 10^16 cm^-2
Atomic Fraction
Depth (nm)
0.14
0.12
0.10
0.08
0.06
0.04
0.02
0.00
0
20
40
60
80
100

Figure 1(b)

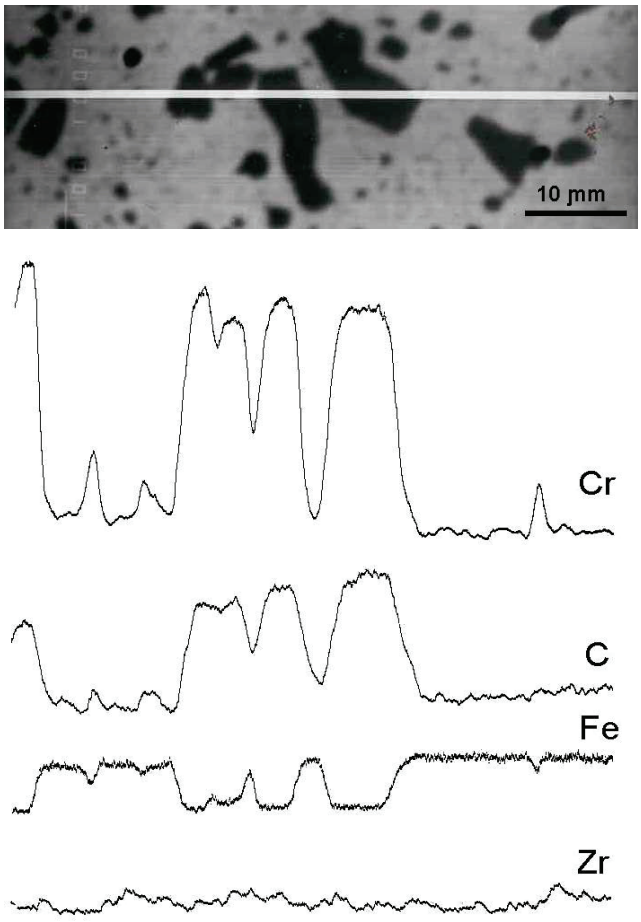

Figure 2

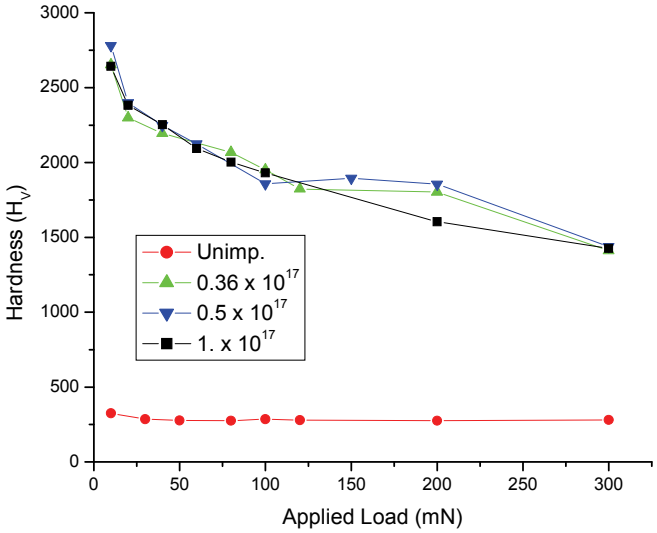
Hardness (H_v)
Applied Load (mN)
Unimp.
0.36 x 10^{17}
0.5 x 10^{17}
1. x 10^{17}
0
500
1000
1500
2000
2500
3000
0
50
100
150
200
250
300

Figure 3

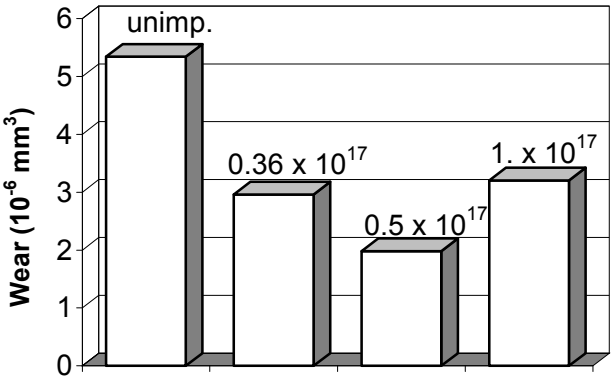

Figure 4